Emergent quantum correlations and collective behavior in non-interacting quantum systems subject to stochastic resetting

Matteo Magoni,[1] Federico Carollo,[1] Gabriele Perfetto,[1] and Igor Lesanovsky[1,2]

[1] *Institut für Theoretische Physik, Eberhard Karls Universität Tübingen, Auf der Morgenstelle 14, 72076 Tübingen, Germany*

[2] *School of Physics and Astronomy and Centre for the Mathematics and Theoretical Physics of Quantum Non-Equilibrium Systems, The University of Nottingham, Nottingham, NG7 2RD, United Kingdom*

(Dated: November 1, 2022)

We investigate the dynamics of a non-interacting spin system, undergoing coherent Rabi oscillations, in the presence of stochastic resetting. We show that resetting generally induces long-range quantum and classical correlations both in the emergent dissipative dynamics and in the non-equilibrium stationary state. Moreover, for the case of conditional reset protocols — where the system is reinitialized to a state dependent on the outcome of a preceding measurement — we show that, in the thermodynamic limit, the spin system can feature collective behavior which results in a phenomenology reminiscent of that occurring in non-equilibrium phase transitions. The discussed reset protocols can be implemented on quantum simulators and quantum devices that permit fast measurement and readout of macroscopic observables, such as the magnetisation. Our approach does not require the control of coherent interactions and may therefore highlight a route towards a simple and robust creation of quantum correlations and collective non-equilibrium states, with potential applications in quantum enhanced metrology and sensing.

Introduction.— Understanding and exploiting the interplay between coherent unitary evolution and measurement in quantum systems has been a central topic since the early days of quantum mechanics [1, 2]. Recent research in this direction is closely linked to the physics of open quantum systems [3–6], where interactions among quantum particles compete with the coupling to the surrounding environment. Modern experiments allow to externally control and even artificially engineer open system dynamics. This can, e.g., be achieved through so-called feedback protocols [7–12], which rely on the continuous monitoring of a system followed by some action conditioned on the output of a detector. This procedure can generate non-equilibrium steady states (NESS) that feature non-trivial quantum correlations [13–16]. Another approach that relies on externally imposed interventions in order to create effectively open system dynamics is *stochastic resetting* [17]. In its simplest form it amounts to resetting a system to its initial state at random times. This procedure has been originally studied for classical diffusive systems [18–21], search processes [18, 19, 22–25] and active systems [26–32], and also here interesting NESS have been shown to emerge [33–44]. Similar observations have been made recently in the context of quantum systems [45–55]. However, it remains an open question whether resetting can induce non-trivial NESS, that may display emergent quantum correlations or even non-equilibrium phase transition behavior.

In this manuscript, we fill this gap by investigating the interplay between stochastic resetting and many-body quantum coherent evolution in the simplest — yet surprisingly non-trivial — case of non-interacting spin systems, see Fig. 1(a). We show that, despite the absence of interactions in the coherent dynamics, resetting induces quantum correlations as well as a critical (non-analytic) behavior in the NESS. We demonstrate this by envisaging three distinct protocols, named henceforth Protocol I, II and III, in increasing order of complexity [see Fig. 1(b,c)]. Protocol I amounts to the aforementioned simple stochastic resetting of the system to a fixed state, while Protocols II and III include a measurement step whose outcome determines to which state the system is reset.

In *all three* cases we find that resetting induces long-range correlations, although the system's reset-free dynamics is non-interacting. These correlations, emerging from the global operations associated with the reset events, are not exclusively of statistical nature but also have a quantum origin. Moreover, Protocols II and III induce stationary collective behavior, which manifests in non-analyticities in an appropriate order parameter. While reminiscent of a non-equilibrium phase transition, the phenomenology we observe here is rather different in nature. Standard phase transitions take place between phases with short-range correlations and finite susceptibility parameter. Here, instead, due to the reset process, the system features strong long-range correlations and a divergent susceptibility throughout the whole phase diagram and not only at the critical point. The collectively enhanced response of the system to external parameter variations may be exploited for high-density quantum sensing, as discussed, e.g., in Ref. [56–58]. The fact that such property emerges even within a simple non-interacting system readily realizable with neutral atoms highlights a novel and simple way for creating and exploiting correlated many-body states on quantum simulators [59–63].

Dynamics and reset states.— We consider a system

of N spins with Hamiltonian

$$H = \Omega \sum_{i=1}^{N} \sigma_i^x + \Delta \sum_{i=1}^{N} \sigma_i^z, \tag{1}$$

describing, for instance, non-interacting atoms subject to an external laser field. Here, $\sigma_i^{x,y,z}$ are the Pauli matrices of the i-th spin, Ω is the Rabi frequency and Δ is the laser detuning. The two basis states of each spin, $|\uparrow\rangle$ and $|\downarrow\rangle$, are chosen as the eigenstates of σ^z and represent the excited state and the ground state, respectively [see Fig. 1(a)]. These can be, for example, two hyper-fine levels of an atom or of an ion.

Before turning to the discussion of the reset protocols, it is useful to first characterize the dynamical properties of the system during its coherent evolution. Since Hamiltonian (1) is the sum of single-body terms, we can focus on the time evolution of single-body operators. For example, the local excitation density at site j, defined as $n_j = (1+\sigma_j^z)/2$, evolves as $n_j^F(t) = e^{iH_j t} n_j e^{-iH_j t}$ with $H_j = \Omega\sigma_j^x + \Delta\sigma_j^z$ and F indicating evolution under the Hamiltonian reset-free dynamics. Without loss of generality, we fix the initial state to be $|\uparrow\rangle^N = \otimes_{i=1}^N |\uparrow\rangle_i$. With this choice one finds $\langle n_j^F(t)\rangle_\uparrow = 1 - (\Omega^2/\overline{\Omega}^2)\sin^2(\overline{\Omega}t)$, where $\overline{\Omega} = \sqrt{\Omega^2+\Delta^2}$ is the effective Rabi frequency and the arrow in the subscript indicates the initial state.

The reset protocols are depicted in Fig. 1(b,c). All have in common that the system evolves coherently with Hamiltonian (1) in between consecutive reset events. In Protocol I, we employ stochastic resetting, i.e., the system is reinitialized to the state $|\uparrow\rangle^N$ unconditionally to any measurement. In Protocols II and III, instead, the reset state is chosen conditionally on a measurement taken right before resetting, as pictured in Fig. 1(c). A natural choice for the quantity to be measured is the excitation density $n = (1/N)\sum_{i=1}^N n_i$. In particular, in Protocol II, first proposed in Ref. [51], two reset states are present, $|\uparrow\rangle^N$ and $|\downarrow\rangle^N$, which correspond to the two completely polarized states with excitation density 1 and 0, respectively. The outcome of the measurement determines the reset state: if the measured excitation density exceeds a certain threshold, which is fixed to be 1/2, then the system is reset to $|\uparrow\rangle^N$, otherwise it is reset to $|\downarrow\rangle^N$. In Protocol III, the system is reset to $|\uparrow\rangle^N$ if the measured density exceeds the threshold. Otherwise, the coherent dynamics resumes from the state obtained by flipping all the spins in the post-measurement configuration, as sketched in Fig. 1(c).

Protocol I: Unconditional reset.— In this simple case the coherent dynamics of the system is interrupted at random times at which the system is reset to state $|\uparrow\rangle^N$. Resets happen at a constant rate γ. The time τ between consecutive reset is therefore distributed according to the Poisson waiting time distribution $f(\tau) = \gamma e^{-\gamma\tau}$ (see Supplemental Material [64] for a different waiting time distribution). The survival probability, i.e., the probability that no reset happens for a time τ, is given by $q(\tau) = \int_\tau^\infty f(s)ds = e^{-\gamma\tau}$. This, together with the reset-free time-evolved density matrix $\rho_\uparrow^F(t)$, determines the quantum state of the system $\rho_\uparrow(t)$ in the presence of resetting through the *last renewal* equation derived in Ref. [48]:

$$\rho_\uparrow(t) = e^{-\gamma t}\rho_\uparrow^F(t) + \gamma\int_0^t dt' e^{-\gamma t'}\rho_\uparrow^F(t'). \tag{2}$$

The first term in the above equation corresponds to having no reset up to time t. The second term accounts for realizations of the stochastic resetting process where the last reset has been at a previous time $t-t'$ and the system has then evolved without reset events up to time t via the Hamiltonian (1).

The average excitation density in the state (2) is given by $\langle n(t)\rangle_\uparrow = \mathrm{Tr}[n\rho_\uparrow(t)]$ and its stationary value reads

$$\langle n\rangle_{\uparrow,\mathrm{ness}} = \lim_{t\to\infty}\langle n(t)\rangle_\uparrow = 1 - 2\frac{\Omega^2}{\gamma^2+4\overline{\Omega}^2}, \tag{3}$$

which is shown in Fig. 2(a). This expression smoothly varies with Ω/Δ contrary to what we will show for Protocols II and III. Equation (3) is equal to 1, i.e., the excitation density of the initial state, for $\Omega = 0$ (no coupling between single spin states), $\gamma\to\infty$ (the infinitely

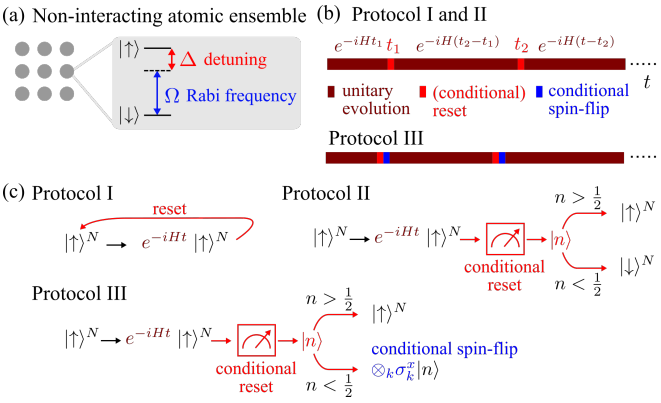

Figure 1. **Non-interacting spins subject to resetting.** (a) Non-interacting spin system subject to a (laser) field with Rabi frequency Ω and detuning Δ. (b) The unitary time evolution according to Hamiltonian (1) is interspersed by randomly distributed reset events, which reinitialize the system to a specific state depending on the adopted reset protocol. In the figure, t denotes the observation time and t_k the time when the k^{th} reset event takes place. (c) Details of the reset protocols. In Protocol I, the system is unconditionally reset to the state $|\uparrow\rangle^N$. In Protocols II and III, the reset is preceded by a measurement of the excitation density n, which selects a product configuration state $|n\rangle$, with density n. In Protocol II, the value of n determines the choice between two fixed reset states. In Protocol III, when $n < 1/2$, the reset state is determined by a spin flip operation applied to the state obtained from the projective measurement.

frequent resets induce a quantum Zeno effect [65, 66] which freezes the system to its initial state) and $\Delta \to \infty$ (transitions between the two spins states are highly off-resonant). Note finally that the limit $\gamma \to 0$ corresponds to a stationary state with extremely rare reset events.

Rather surprisingly, although in each realization of the process the system is in a product state at all times, the reset mechanism introduces long-range correlations. This is due to the *global* character of the resetting procedure: all the individual spins are reset to the same single-spin state. This becomes evident when looking at the stationary two-spin connected correlation function $C^{\uparrow}_{jk} = \left[\langle n_j n_k\rangle_{\uparrow,\mathrm{ness}} - \langle n_j\rangle_{\uparrow,\mathrm{ness}} \langle n_k\rangle_{\uparrow,\mathrm{ness}}\right]$, which is equal to

$$C^{\uparrow}_{jk} = 4\Omega^4 \frac{5\gamma^2 + 8\overline{\Omega}^2}{\left(\gamma^2 + 4\overline{\Omega}^2\right)^2 \left(\gamma^2 + 16\overline{\Omega}^2\right)}, \tag{4}$$

showing that correlations do not depend on the considered spins. This is reminiscent of what happens in fully connected models (see, e.g., [67] for an example in dissipative settings). However, in our case, these correlations are *strong* in the sense that they do not vanish in the thermodynamic $N \to \infty$ limit. As such, contrary to the case of fully connected models [68], the stationary state of our reset process is not clustering, i.e., it does not possess Gaussian fluctuations, as shown by the fact that the susceptibility is diverging: $\chi = \lim_{N\to\infty} 1/N \sum_{j,k=1}^{N} C^{\uparrow}_{jk} = \infty$. Note, that the correlations (4) can also be computed from suitable single-spin trajectory correlations, following, e.g., Ref. [69]. This is, however, not possible for Hamiltonians with interactions among the spins or for the protocols II and III discussed further below.

In addition to these strong classical density-density correlations, the NESS, in fact, also contains correlations of quantum origin. This aspect can be shown by computing the local quantum uncertainty (LQU), defined in Ref. [70], which is a type of bipartite quantum discord [71, 72]. It quantifies the extent of the fluctuations of a local measurement due to the non-commutativity between the state and the measured local observable. The LQU isolates the fluctuations that are caused only by the coherence of the state and not by its mixedness. Despite being a fairly common feature in quantum states [73], quantum discord is proved to be a useful quantity for metrology and sensing applications [74–76] . Here we compute the LQU for the stationary two-spin reduced density matrix ρ_{jk} [64]. It is given by $l_{jk} = 1 - \lambda_{\max}\{W_{jk}\}$, where $\lambda_{\max}\{W_{jk}\}$ is the largest eigenvalue of the 3×3 matrix W_{jk} with elements $\left(W_{jk}\right)_{ab} = \mathrm{Tr}[\sqrt{\rho_{jk}}(\sigma^a_j \otimes \mathbb{1})\sqrt{\rho_{jk}}(\sigma^b_j \otimes \mathbb{1})]$, with $a, b = x, y, z$. As for the classical correlations, also the LQU does not depend on the distance between sites. In Fig. 2(d) we show the connected correlation function (4) (left axis) together with the quantum discord quantified via the LQU (right axis) for Protocol I. Both quantities possess qualitatively the same shape and smoothly vary with Ω/Δ.

Protocol II: Conditional reset to two states.— This protocol exploits two reset states: $|\uparrow\rangle^N$ and $|\downarrow\rangle^N$. At each reset event, the local density at each site is measured and the total excitation density n is computed. The system is reinitialized to the reset state $|\uparrow\rangle^N$ if the majority of the spins is found in the excited state, i.e., $n > 1/2$. On the contrary, if $n < 1/2$, the reset state is chosen as $|\downarrow\rangle^N$. For large N, the probability distribution for measuring a certain value of n after a time t since the last reset is a Gaussian distribution centered on the average $\langle n^F(t)\rangle_{\uparrow/\downarrow}$, with variance $\sigma^2_n \propto 1/N$ [64]. This means that, at each reset event, the system can in principle be reinitialized in both reset states, albeit with different probabilities. This aspect, together with the fact that the Hamiltonian dynamics of the average density satisfies the relation $\langle n^F(t)\rangle_{\uparrow} = 1 - \langle n^F(t)\rangle_{\downarrow}$, makes the stationary excitation density exactly equal to $1/2$, i.e., the average between the density of the two reset states [64].

A different phenomenology takes place in the thermodynamic limit $N \to \infty$. In this case, as a consequence of the *law of large numbers* applied to the operator n, the probability distribution to measure a certain value for n becomes a delta-function peaked around the average $\langle n^F(t)\rangle_{\uparrow/\downarrow}$. This self-averaging property makes the measurement of the excitation density fully deterministic with outcome equal to its average value. As a consequence, for $\Omega < \Delta$, given the initial condition and the fact that $\langle n^F(t)\rangle_{\uparrow} > 1/2 \ \ \forall t$, the system can only be reset to the state $|\uparrow\rangle^N$ and, therefore, the average density in the process is always larger than $1/2$. For $\Omega > \Delta$, instead, both reset states can be reached so that the stationary excitation density is equal to $1/2$ [64]. The stationary excitation density, acting as an order parameter, then displays a jump discontinuity at the critical point $\Omega_c = \Delta$, as shown in Fig. 2(b). This is a consequence of an abrupt change in the dynamics: for $\Omega > \Delta$ the system can reset to both states, while for $\Omega < \Delta$ the dynamics is effectively that of Protocol I, with the stationary excitation density coinciding with Eq. (3) [see also Fig. 2].

As shown in Fig. 2(e) the connected correlation function and the quantum discord display a behavior that is qualitatively different to that of Protocol I. They are both discontinuous at the critical point even though the discontinuity of the LQU is tiny on the scale of the figure.

Protocol III: Conditional reset to the initial state.— In the third protocol, the system is reset to its initial state $|\uparrow\rangle^N$ only if the measured excitation density exceeds $1/2$. If not, the system resumes its dynamics from the state generated by the projective measurement after a subsequent flip of all its spins is performed [see Fig. 1(b,c)]. This means that, if the state after the projective measurement possesses an excitation density equal to $n' < 1/2$, the reset state will have excitation density

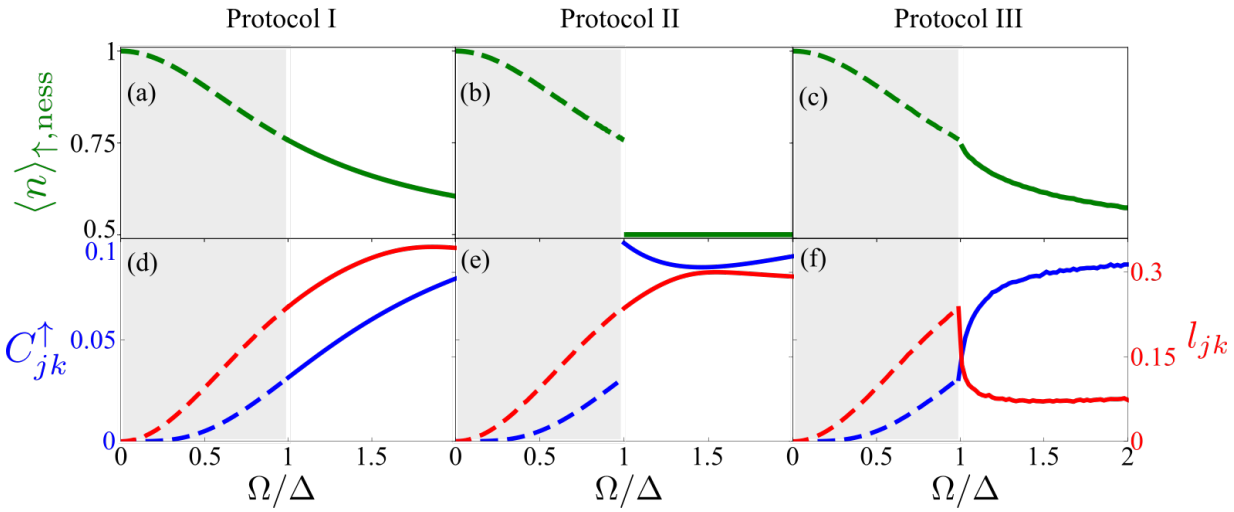

Figure 2. **Collective behavior and quantum correlations induced by reset.** First row: stationary excitation density as a function of Ω/Δ for the three protocols. (a) For Protocol I the order parameter (excitation density) is given by Eq. (3). For Protocols II (b) and III (c), the order parameter displays a non-analyticity at the critical point $\Omega_c = \Delta$, which is discontinuous or continuous, respectively. For protocol III the order parameter behaves as a power law when approaching the critical point from the right with an exponent close to 0.5. Second row: connected correlation function (in blue, left axis) and quantum discord (in red, right axis), computed from the two-spin reduced density matrix ρ_{jk}, as a function of Ω/Δ. In contrast to Protocol I (d), where both quantities are continuous, Protocol II (e), leads to a discontinuity of both quantities at the critical point $\Omega_c = \Delta$. Note, that the discontinuity of the quantum discord is imperceptible on the scale shown. (f) For reset Protocol III, both the connected correlation function and the quantum discord feature power-law behavior in a right neighborhood of the critical point. The characteristic exponent is approximately 0.5 for the connected correlation function and 0.2 for the quantum discord. The dashed parts of the curves in all panels highlight the fact that, when $\Omega < \Delta$, the three protocols become equivalent. All data are obtained analytically, except for panels (c) and (f) where numerical simulations are necessary. The reset rate is chosen to be $\gamma = \Delta/2$.

$1 - n' > 1/2$. This protocol is still conditioned on the measured excitation density, but, in contrast to Protocol II, any state with $n > 1/2$ can be considered as a reset state according to the parameter regime. The resulting non-equilibrium phase diagram, see Fig. 2(c), exhibits a continuous non-analytic behavior at the critical point $\Omega_c = \Delta$.

We note that, without the additional spin-flip operation, the stationary behavior of the density would be discontinuous also for this protocol. Indeed, when $\Omega > \Delta$, each realization of the reset process would spend on average half of the time in configurations with n smaller than $1/2$ and half of the time in configurations with n larger than $1/2$. The stationary state, obtained by averaging over trajectories, would therefore be very different from the one attained when $\Omega < \Delta$, where trajectories maintain a positive magnetization, $n > 1/2$, throughout the whole reset process. This substantial dissimilarity between the two regimes would result in a jump discontinuity of the order parameter at Ω_c. On the contrary, with the introduction of the spin-flip operation, the order parameter is continuous, but still non-analytic, since its first derivative has a jump discontinuity at Ω_c. This can be understood by noticing that, in this case, for $\Omega \gtrsim \Delta$ each trajectory of the reset process spends only an infinitesimal time in states with $n < 1/2$, since after a reset the system restarts the dynamics from a state with $n > 1/2$.

In the vicinity of Ω_c, the order parameter displays a power-law behaviour $\sim (\Omega - \Omega_c)^{\beta}$, for $\Omega \to \Omega_c^{+}$, with a static exponent $\beta \approx 0.5$. This seems to indicate the emergence of a second-order phase transition in the NESS. However, looking at the behavior of the correlation function reveals a rather unexpected phenomenology. Indeed, in second-order phase transitions, upon approaching the critical point, the correlation length of the system increases giving rise to a power-law divergence of the susceptibility at criticality. Here, instead, as mentioned already when discussing Protocol I, the system features strong long-range correlations which determine a divergence of the susceptibility parameter χ for any value of Ω/Δ and not only at criticality. Despite this divergence, we can still analyse the two-spin correlation function $C^{\uparrow}_{jk}$. This quantity, displayed in Fig. 2(f), interestingly also obeys a power-law behaviour $\sim (\Omega - \Omega_c)^{\beta}$ close to the critical point, with the same static exponent β of the order parameter. Also the quantum discord, as measured by the LQU, follows a power law with exponent $\delta \approx 0.2$.

Conclusions and outlook.— We have shown that combining a non-interacting quantum dynamics with an externally imposed reset process can lead to surprisingly rich non-equilibrium stationary states. Even the simplest possible protocol results in a state with non-trivial classi-

cal and quantum correlations. More involved protocols lead to the emergence of a phase-transition behavior in an initially non-interacting system, which may be relevant for the implementation of quantum sensing and metrology applications [56, 77–79]. The non-analyticities characterizing such collective behavior emerge since the reset state is completely determined, in the thermodynamic limit, by the average value of the density as a consequence of the *law of large numbers*. For any finite system, fluctuations in the measurement outcomes inhibit the emergence of the observed non-analyticities. We have shown how this occurs in the case of a non-interacting unitary dynamics. However, one would observe a similar phenomenology in the case of Hamiltonian dynamics with short-range interactions, for which the time-evolution only builds up exponentially decaying correlations which do not invalidate the convergence of the operator n to its average value, in the large N limit. Conceptually, this mechanism underlying collective behavior may appear simpler than the creation of strong coherent interactions. However, one requires the ability to rapidly read out and initialize the spin ensemble [80]. For the results discussed in Fig. 2 we have assumed a reset rate $\gamma = \Delta/2$, which in some settings may be impractical (it could be on the order of MHz for cold atoms). However, our findings do not change qualitatively for smaller values of the reset rate. The key quantity is indeed the ratio Ω/Δ, while the value of γ simply provides the timescale for the approach to stationarity.

Acknowledgements.— We acknowledge support from the "Wissenschaftler Rückkehrprogramm GSO/CZS" of the Carl-Zeiss-Stiftung and the German Scholars Organization e.V., from the European Union's Horizon 2020 research and innovation program under Grant Agreement No. 800942 (ErBeStA), as well as from the Baden-Württemberg Stiftung through Project No. BWST_ISF2019-23. We also acknowledge funding from the Deutsche Forschungsgemeinschaft through SPP 1929 (GiRyd), Grant No. 428276754, as well as through the Research Unit FOR 5413/1, Grant No. 465199066. G.P. acknowledges support from the Alexander von Humboldt Foundation through a Humboldt research fellowship for postdoctoral researchers.

[1] M. Born, Quantenmechanik der Stoßvorgänge, Z. Physik **38**, 803 (1926).
[2] N. Bohr, The Quantum Postulate and the Recent Development of Atomic Theory, Nature **121**, 580 (1928).
[3] G. Lindblad, On the generators of quantum dynamical semigroups, Commun. Math. Phys. **48**, 119 (1976).
[4] V. Gorini, A. Kossakowski, and E. C. G. Sudarshan, Completely positive dynamical semigroups of N-level systems, J. Math. Phys. **17**, 821 (1976).
[5] C. Gardiner and P. Zoller, *Quantum Noise: a handbook of Markovian and non-Markovian quantum stochastic methods with applications to quantum optics*, Springer Series in Synergetics (Springer, 2004).
[6] H.-P. Breuer and F. Petruccione, *The Theory of Open Quantum Systems* (Oxford University Press, Oxford, 2007).
[7] H. M. Wiseman, Quantum theory of continuous feedback, Phys. Rev. A **49**, 2133 (1994).
[8] H. M. Wiseman and G. J. Milburn, *Quantum Measurement and Control* (Cambridge University Press, 2009).
[9] K. Jacobs, *Quantum Measurement Theory and its Applications* (Cambridge University Press, 2014).
[10] J. Lammers, H. Weimer, and K. Hammerer, Open-system many-body dynamics through interferometric measurements and feedback, Phys. Rev. A **94**, 052120 (2016).
[11] H. Nurdin and N. Yamamoto, *Linear Dynamical Quantum Systems: Analysis, Synthesis, and Control* (Springer International Publishing, 2017).
[12] K. Kroeger, N. Dogra, R. Rosa-Medina, M. Paluch, F. Ferri, T. Donner, and T. Esslinger, Continuous feedback on a quantum gas coupled to an optical cavity, New J. Phys. **22**, 033020 (2020).
[13] D. A. Ivanov, T. Y. Ivanova, S. F. Caballero-Benitez, and I. B. Mekhov, Feedback-Induced Quantum Phase Transitions Using Weak Measurements, Phys. Rev. Lett. **124**, 010603 (2020).
[14] G. Buonaiuto, F. Carollo, B. Olmos, and I. Lesanovsky, Dynamical phases and quantum correlations in an emitter-waveguide system with feedback, Phys. Rev. Lett. **127**, 133601 (2021).
[15] D. A. Ivanov, T. Y. Ivanova, S. F. Caballero-Benitez, and I. B. Mekhov, Tuning the universality class of phase transitions by feedback: Open quantum systems beyond dissipation, Phys. Rev. A **104**, 033719 (2021).
[16] J. T. Young, A. V. Gorshkov, and I. B. Spielman, Feedback-stabilized dynamical steady states in the Bose-Hubbard model, Phys. Rev. Research **3**, 043075 (2021).
[17] M. R. Evans, S. N. Majumdar, and G. Schehr, Stochastic resetting and applications, J. Phys. A: Math. Theor. **53**, 193001 (2020).
[18] M. R. Evans and S. N. Majumdar, Diffusion with Stochastic Resetting, Phys. Rev. Lett. **106**, 160601 (2011).
[19] M. R. Evans and S. N. Majumdar, Diffusion with optimal resetting, J. Phys. A: Math. Theor. **44**, 435001 (2011).
[20] M. R. Evans and S. N. Majumdar, Diffusion with resetting in arbitrary spatial dimension, J. Phys. A: Math. Theor. **47**, 285001 (2014).
[21] S. N. Majumdar, S. Sabhapandit, and G. Schehr, Dynamical transition in the temporal relaxation of stochastic processes under resetting, Phys. Rev. E **91**, 052131 (2015).
[22] L. Kusmierz, S. N. Majumdar, S. Sabhapandit, and G. Schehr, First Order Transition for the Optimal Search Time of Lévy Flights with Resetting, Phys. Rev. Lett. **113**, 220602 (2014).
[23] A. Pal and S. Reuveni, First Passage under Restart, Phys. Rev. Lett. **118**, 030603 (2017).
[24] A. Chechkin and I. M. Sokolov, Random Search with Resetting: A Unified Renewal Approach, Phys. Rev. Lett. **121**, 050601 (2018).
[25] M. Radice, Diffusion processes with Gamma-distributed resetting and non-instantaneous returns, J. Phys. A: Math. Theor. **55**, 224002 (2022).
[26] M. R. Evans, S. N. Majumdar, and K. Mallick, Optimal diffusive search: nonequilibrium resetting versus equilib-

rium dynamics, J. Phys. A: Math. Theor. **46**, 185001 (2013).
[27] C. Christou and A. Schadschneider, Diffusion with resetting in bounded domains, J. Phys. A: Math. Theor. **48**, 285003 (2015).
[28] A. B. Slowman, M. R. Evans, and R. A. Blythe, Jamming and Attraction of Interacting Run-and-Tumble Random Walkers, Phys. Rev. Lett. **116**, 218101 (2016).
[29] M. R. Evans and S. N. Majumdar, Run and tumble particle under resetting: a renewal approach, J. Phys. A: Math. Theor. **51**, 475003 (2018).
[30] V. Kumar, O. Sadekar, and U. Basu, Active Brownian motion in two dimensions under stochastic resetting, Phys. Rev. E **102**, 052129 (2020).
[31] I. Santra, U. Basu, and S. Sabhapandit, Run-and-tumble particles in two dimensions under stochastic resetting conditions, J. Stat. Mech. **2020**, 113206 (2020).
[32] P. C. Bressloff, Modeling active cellular transport as a directed search process with stochastic resetting and delays, J. Phys. A: Math. Theor. **53**, 355001 (2020).
[33] S. Gupta, S. N. Majumdar, and G. Schehr, Fluctuating Interfaces Subject to Stochastic Resetting, Phys. Rev. Lett. **112**, 220601 (2014).
[34] S. Eule and J. J. Metzger, Non-equilibrium steady states of stochastic processes with intermittent resetting, New J. Phys. **18**, 033006 (2016).
[35] V. Méndez and D. Campos, Characterization of stationary states in random walks with stochastic resetting, Phys. Rev. E **93**, 022106 (2016).
[36] P. Grange, Non-conserving zero-range processes with extensive rates under resetting, J. Phys. Commun. **4**, 045006 (2020).
[37] M. Magoni, S. N. Majumdar, and G. Schehr, Ising model with stochastic resetting, Phys. Rev. Research **2**, 033182 (2020).
[38] C. Aron and M. Kulkarni, Nonanalytic nonequilibrium field theory: Stochastic reheating of the Ising model, Phys. Rev. Research **2**, 043390 (2020).
[39] W. Wang, A. G. Cherstvy, H. Kantz, R. Metzler, and I. M. Sokolov, Time averaging and emerging nonergodicity upon resetting of fractional Brownian motion and heterogeneous diffusion processes, Phys. Rev. E **104**, 024105 (2021).
[40] V. Stojkoski, T. Sandev, L. Kocarev, and A. Pal, Geometric Brownian motion under stochastic resetting: A stationary yet nonergodic process, Phys. Rev. E **104**, 014121 (2021).
[41] I. Santra, S. Das, and S. K. Nath, Brownian motion under intermittent harmonic potentials, J. Phys. A: Math. Theor. **54**, 334001 (2021).
[42] F. Huang and H. Chen, Random walks on complex networks with first-passage resetting, Phys. Rev. E **103**, 062132 (2021).
[43] K. Goswami and R. Chakrabarti, Stochastic resetting and first arrival subjected to Gaussian noise and Poisson white noise, Phys. Rev. E **104**, 034113 (2021).
[44] P. Chelminiak, Non-linear diffusion with stochastic resetting, arXiv:2107.14680 (2021).
[45] L. Hartmann, W. Dür, and H.-J. Briegel, Steady-state entanglement in open and noisy quantum systems, Phys. Rev. A **74**, 052304 (2006).
[46] N. Linden, S. Popescu, and P. Skrzypczyk, How Small Can Thermal Machines Be? The Smallest Possible Refrigerator, Phys. Rev. Lett. **105**, 130401 (2010).
[47] A. Tavakoli, G. Haack, N. Brunner, and J. B. Brask, Autonomous multipartite entanglement engines, Phys. Rev. A **101**, 012315 (2020).
[48] B. Mukherjee, K. Sengupta, and S. N. Majumdar, Quantum dynamics with stochastic reset, Phys. Rev. B **98**, 104309 (2018).
[49] D. C. Rose, H. Touchette, I. Lesanovsky, and J. P. Garrahan, Spectral properties of simple classical and quantum reset processes, Phys. Rev. E **98**, 022129 (2018).
[50] F. Carollo, R. L. Jack, and J. P. Garrahan, Unraveling the Large Deviation Statistics of Markovian Open Quantum Systems, Phys. Rev. Lett. **122**, 130605 (2019).
[51] G. Perfetto, F. Carollo, M. Magoni, and I. Lesanovsky, Designing nonequilibrium states of quantum matter through stochastic resetting, Phys. Rev. B **104**, L180302 (2021).
[52] A. Riera-Campeny, J. Ollé, and A. Masó-Puigdellosas, Measurement-induced resetting in open quantum systems, arXiv:2011.04403 (2020).
[53] X. Turkeshi, M. Dalmonte, R. Fazio, and M. Schirò, Entanglement Transitions from Stochastic Resetting of Non-Hermitian Quasiparticles, arXiv:2111.03500 (2021).
[54] D. Das, S. Dattagupta, and S. Gupta, Quantum unitary evolution interspersed with repeated non-unitary interactions at random times: the method of stochastic Liouville equation, and two examples of interactions in the context of a tight-binding chain, J. Stat. Mech. **2022**, 053101 (2022).
[55] G. Perfetto, F. Carollo, and I. Lesanovsky, Thermodynamics of quantum-jump trajectories of open quantum systems subject to stochastic resetting, arXiv:2112.05078 (2021).
[56] M. Raghunandan, J. Wrachtrup, and H. Weimer, High-Density Quantum Sensing with Dissipative First Order Transitions, Phys. Rev. Lett. **120**, 150501 (2018).
[57] L.-P. Yang and Z. Jacob, Quantum critical detector: amplifying weak signals using discontinuous quantum phase transitions, Opt. Express **27**, 10482 (2019).
[58] Y. Chu, S. Zhang, B. Yu, and J. Cai, Dynamic Framework for Criticality-Enhanced Quantum Sensing, Phys. Rev. Lett. **126**, 010502 (2021).
[59] I. M. Georgescu, S. Ashhab, and F. Nori, Quantum simulation, Rev. Mod. Phys. **86**, 153 (2014).
[60] M. Endres, H. Bernien, A. Keesling, H. Levine, E. Anschuetz, A. Krajenbrink, C. Senko, V. Vuletic, M. Greiner, and M. Lukin, Atom-by-atom assembly of defect-free one-dimensional cold atom arrays, Science **354** (2016).
[61] D. Barredo, S. Léséleuc, V. Lienhard, T. Lahaye, and A. Browaeys, An atom-by-atom assembler of defect-free arbitrary 2D atomic arrays, Science **354** (2016).
[62] C. Robens, J. Zopes, W. Alt, S. Brakhane, D. Meschede, and A. Alberti, Low-Entropy States of Neutral Atoms in Polarization-Synthesized Optical Lattices, Phys. Rev. Lett. **118**, 065302 (2017).
[63] L. Henriet, L. Beguin, A. Signoles, T. Lahaye, A. Browaeys, G.-O. Reymond, and C. Jurczak, Quantum computing with neutral atoms, Quantum **4**, 327 (2020).
[64] See Supplemental Material for details of the calculations.
[65] B. Misra and E. C. G. Sudarshan, The Zeno's paradox in quantum theory, J. Math. Phys. **18**, 756 (1977).
[66] C. B. Chiu, E. C. G. Sudarshan, and B. Misra, Time evolution of unstable quantum states and a resolution of Zeno's paradox, Phys. Rev. D **16**, 520 (1977).
[67] F. Benatti, F. Carollo, R. Floreanini, and H. Narnhofer, Quantum spin chain dissipative mean-field dynamics, J. Phys. A: Math. Theor. **51**, 325001 (2018).

[68] F. Benatti, F. Carollo, R. Floreanini, and H. Narnhofer, Non-markovian mesoscopic dissipative dynamics of open quantum spin chains, Phys. Lett. A **380**, 381 (2016).
[69] M. Buchhold, Y. Minoguchi, A. Altland, and S. Diehl, Effective Theory for the Measurement-Induced Phase Transition of Dirac Fermions, Phys. Rev. X **11**, 041004 (2021).
[70] D. Girolami, T. Tufarelli, and G. Adesso, Characterizing Nonclassical Correlations via Local Quantum Uncertainty, Phys. Rev. Lett. **110**, 240402 (2013).
[71] H. Ollivier and W. H. Zurek, Quantum Discord: A Measure of the Quantumness of Correlations, Phys. Rev. Lett. **88**, 017901 (2001).
[72] L. Henderson and V. Vedral, Classical, quantum and total correlations, J. Phys. A: Math. Gen. **34**, 6899 (2001).
[73] A. Ferraro, L. Aolita, D. Cavalcanti, F. M. Cucchietti, and A. Acín, Almost all quantum states have nonclassical correlations, Phys. Rev. A **81**, 052318 (2010).
[74] K. Modi, H. Cable, M. Williamson, and V. Vedral, Quantum Correlations in Mixed-State Metrology, Phys. Rev. X **1**, 021022 (2011).
[75] D. Girolami, A. M. Souza, V. Giovannetti, T. Tufarelli, J. G. Filgueiras, R. S. Sarthour, D. O. Soares-Pinto, I. S. Oliveira, and G. Adesso, Quantum Discord Determines the Interferometric Power of Quantum States, Phys. Rev. Lett. **112**, 210401 (2014).
[76] A. Sone, Q. Zhuang, and P. Cappellaro, Quantifying precision loss in local quantum thermometry via diagonal discord, Phys. Rev. A **98**, 012115 (2018).
[77] C. G. Wade, M. Marcuzzi, E. Levi, J. M. Kondo, I. Lesanovsky, C. S. Adams, and K. J. Weatherill, A terahertz-driven non-equilibrium phase transition in a room temperature atomic vapour, Nat. Commun. **9**, 3567 (2018).
[78] Y.-Y. Jau and T. Carter, Vapor-Cell-Based Atomic Electrometry for Detection Frequencies below 1 kHz, Phys. Rev. Applied **13**, 054034 (2020).
[79] L. A. Downes, A. R. MacKellar, D. J. Whiting, C. Bourgenot, C. S. Adams, and K. J. Weatherill, Full-Field Terahertz Imaging at Kilohertz Frame Rates Using Atomic Vapor, Phys. Rev. X **10**, 011027 (2020).
[80] S. Hollerith, J. Zeiher, J. Rui, A. Rubio-Abadal, V. Walther, T. Pohl, D. M. Stamper-Kurn, I. Bloch, and C. Gross, Quantum gas microscopy of Rydberg macrodimers, Science **364**, 664 (2019).